Multiuser Communications for Underwater Acoustic Networks using MIMO-OFDM-IDMA

Lance Linton, Phillip Conder, and Michael Faulkner
Centre for Telecommunications and Micro-Electronics (CTME),
Victoria University, Melbourne, Australia
Email: lance.linton@live.vu.edu.au, {phillip.conder, mike.faulkner}@vu.edu.au

***Abstract*—In this paper, we present MIMO-OFDM-IDMA, a novel multiple-access communications scheme that provides robust performance in the presence of large time-delay spread and the other channel impairments commonly encountered in shallow water acoustic networks. MIMO-OFDM-IDMA is a multiple-input multiple-output system that employs orthogonal frequency division multiplexing scheme with an IDMA overlay, where IDMA is a variant of code-division multiple access (CDMA). Simulation results show that the MIMO-OFDM-IDMA scheme outperforms other common multiple-access schemes in the shallow water acoustic network environment.**

I. INTRODUCTION

The shallow water acoustic channel is an exceptionally difficult medium for data transmission, and developing reliable communications systems for this environment has proved to be very challenging. One of the main channel impairments is multipath interference caused by multiple reflections of the acoustic signal from the water surface and bottom. These reflections occur at small grazing angles and with small reflection losses. This effect causes both long time-delay spread and large multipath amplitudes to be present in the received signal [1].

Over the past decade, CDMA has been successfully employed as the modulation scheme for shallow water networks [2] [3] [4]. CDMA is a spread-spectrum technique that can provide simultaneous access for multiple users. Spread-spectrum schemes employ a transmission bandwidth that is considerably greater than the information rate. Utilization of the bandwidth in this manner introduces a number of benefits, including multiple-access interference suppression capability and improved immunity against multipath effects.

In a CDMA scheme, spreading codes or signatures are used to distinguish between users. The spreading codes also allow transmission between users to occur within the same frequency band and time slot. This allows users to randomly access the channel and is an important feature of the scheme.

Unfortunately, the long time-delay spreads that are typical for shallow water acoustic channels cause severe inter-symbol interference (ISI). This ISI degrades the performance of many CDMA receiver detection schemes.

However, OFDM is a modulation scheme that is particularly resilient to long time-delay spreads. The basic principle of OFDM is to split a high-rate data stream into a number of lower-rate streams that are transmitted simultaneously over a number of sub-carriers. Because the symbol duration increases for the lower-rate parallel sub-carriers, the relative amount of dispersion in time caused by time-delay spread is significantly reduced.

Recently, a new multiple access system, IDMA has been proposed [5]. IDMA when used with low-complexity iterative receivers has been shown to outperform coded CDMA in wireless applications. In contrast to CDMA, which separates users by specific spreading codes, IDMA separates users by unique interleaver sequences. IDMA can be regarded as a special case of chip interleaved CDMA, and inherits many of the advantages of CDMA [6].

In this paper, we combine OFDM with an IDMA overlay to develop a multiple-access communications system that provides robust performance in the presence of large time-delay spread and the other impairments presented by the shallow water acoustic channel. The proposed OFDM-IDMA scheme utilises a low-complexity iterative decoding algorithm based on the turbo-decoding concept [7].

The performance of the proposed OFMD-IDMA scheme is compared against other shallow water communication schemes, including single-carrier CDMA, single-carrier IDMA. Using ray-trace underwater channel models combined with noise models of commonly occurring oceanic noise phenomena, simulations of multiuser systems are performed to assess the overall performance of the different schemes.

A Multiple-Input Multiple-Output (MIMO) extension to the OFDM-IDMA scheme is also investigated. MIMO is a general term that refers to communication schemes where each transmitter and receiver use multiple transmitting and receiving elements respectively. This MIMO concept is used to exploit the multi-path nature of the underwater channel to provide improved performance in the form of either increased data robustness or increased data throughput.

II. CHANNEL MODEL

Acoustic signals transmitted in shallow water are corrupted by interference from reflection and scattering at the water surface and bottom. For this reason, the shallow water channel is a difficult medium in which to achieve the high data rates needed for many applications. An especially difficult problem is that the acoustic signal transmitted over a shallow water channel has associated with it inherently small grazing angles and small reflection losses. This results in significant corruption due to large amplitude multi-path signals.

978-1-4244-4242-3/08/$25.00 ©2008 IEEE

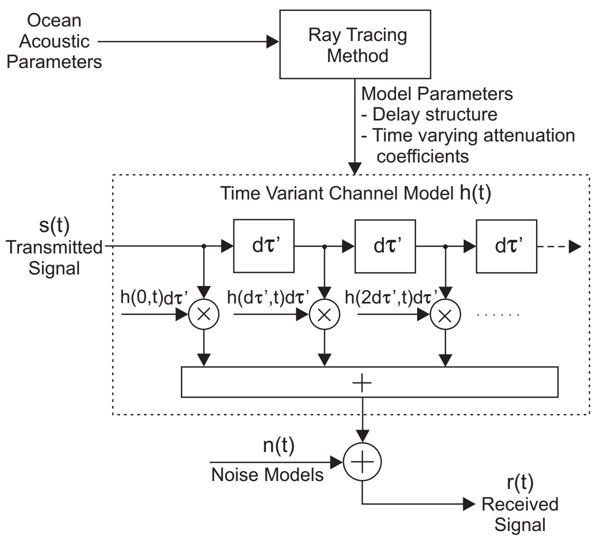

Fig. 1. Channel Model Simulator Description

Channel models based on ray tracing methods have been shown to provide realistic modeling of high frequency acoustic signals propagating in shallow water environments [8].

The channel model used for the system simulations is shown in Fig 1. We use a ray-trace underwater channel model combined with noise models of commonly occurring oceanic noise phenomena (surface agitation noise, thermal noise, rain noise, and noise due to snapping shrimp).

A. Multipath Modeling

The shallow water propagation is modeled using the multipath model proposed by Zielinski, Yoon and Wu [9]. This channel model is characterised by Ray theory (simplified due to constant sound velocity profile and constant bottom depth assumptions) and extending it to a multipath expansion for a series of reflections resulting in multipath arrivals at the receiver.

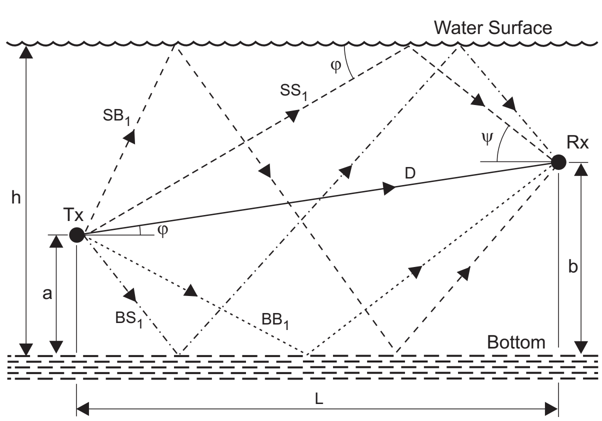

Fig. 2. Multipath structure of a shallow water channel

Boundaries at the channel surface and bottom reflect an acoustic signal, resulting in multiple travel paths between transmitter and receiver. The receiver can thus acquire signals arriving on different paths, each signal delayed according to the channel geometry. In this paper, we assume a channel geometry as shown in Fig 2. The channel has uniform depth h and constant sound speed c. The transmitter and receiver height are denoted by a, and b respectively.

We only consider the case where the channel has a large range to channel depth ratio (L/h), such that it supports coherent, specular reflection.

The transmitted signal path can be classified as either the direct path D or multipath. Multipath signals are grouped into four types according to their first and last boundary reflection before arriving at the receiver. We use the following notation:

- SS denotes a multipath signal which has a first and last boundary reflection from the sea-surface;
- SB denotes a multipath signal which has first and last boundary reflections from the sea surface and bottom respectively;
- BS denotes a multipath signal which has first and last boundary reflections from the sea bottom and surface respectively; and
- BB to denote multipath signals which make a first and last boundary reflection from the sea bottom.

We extend this notation to define a given order of multipath by writing SS_n, SB_n, BS_n, BB_n, where the subscript n denotes the multipath "order". Multipath signals with an order, n, of 2 or more have an additional $(n-1)$ intermediatory boundary reflections. These four types of multipath signals are shown in Fig 2 for the primary, $n = 1$, path.

Calculation of the combined response of received direct and reflected path signals can be performed by the summation of image signals.

The impulse response of a multi-path channel can be modeled by the weighted sum of delayed delta functions [10]. The received signal $r(t)$ can therefore be represented by a weighted sum of the delayed transmitted signal $s(t)$, that is:

$$r(t) = \sum_{i=1}^{\infty} \alpha_i s(t - \tau_i) \tag{1}$$

where α_i is the amplitude of the signal received from the i-th path normalised by the amplitude of the direct path signal (i = 1), and τ_i designates the difference in time of arrivals between the direct path signal $(i = 1)$ and reflected signals $(i \neq 1)$.

1) Multipath Signal Amplitude Calculation: The normalised amplitudes of each of the four types of multipath signals can be calculated from the following:

$$\alpha_{SS_n} = [\frac{D}{SS_n}]R_{SS_n}, \qquad \alpha_{SB_n} = [\frac{D}{SB_n}]R_{SB_n},$$
$$\alpha_{BS_n} = [\frac{D}{BS_n}]R_{BS_n}, \qquad \alpha_{BB_n} = [\frac{D}{BB_n}]R_{BB_n} \tag{2}$$

where D, SS_n, SB_n, BS_n, BB_n are the lengths of the signal paths; and R_{SS_n}, R_{SB_n}, R_{BS_n}, R_{BB_n} are the combined attenuation due to repeated surface and/or bottom reflections for each type of multipath.

The path lengths can be calculated using the channel geometry. Using the binomial expansion to simplify the equations, the path lengths for the direct signal and each of the multipath types is given by:

$$\begin{aligned}
D &\simeq [L + \frac{1}{2L}(b-a)^2] \\
SS_n &\simeq [L + \frac{1}{2L}(2nh-a-b)^2] \\
SB_n &\simeq [L + \frac{1}{2L}(2nh-a+b)^2] \\
BS_n &\simeq [L + \frac{1}{2L}(2nh+a-b)^2] \\
BB_n &\simeq [L + \frac{1}{2L}(2(n-1)h+a+b)^2] \qquad (3)
\end{aligned}$$

The combined attenuation due to repeated surface and/or bottom reflections is given by

$$\begin{aligned}
R_{SS_n} &= \tilde{r}_s^n \tilde{r}_b^{n-1} \simeq -|r_s|^n \\
R_{SB_n} &= \tilde{r}_s^n \tilde{r}_b^n \simeq |r_s|^n \\
R_{BS_n} &= \tilde{r}_s^n \tilde{r}_b^n \simeq |r_s|^n \\
R_{BB_n} &= \tilde{r}_s^{n-1} \tilde{r}_b^n \simeq -|r_s|^{n-1} \qquad (4)
\end{aligned}$$

The surface reflection coefficient, r_s can be evaluated using the Bechmann-Spezzichino model, and the bottom reflection coefficient, r_b can be evaluated using either the Rayleigh model (Brekhovskikh) or the NUSC model (Yarger) [9]. In general, reflection coefficients depend on grazing angle and therefore on the order of the multipath.

2) Multipath Signal Arrival Time Calculation: The difference in arrival times between the direct path and each of the four types of multipath signals can be calculated from the following:

$$\begin{aligned}
\tau_{SS_n} &\simeq \frac{2}{Lc}[n^2h^2 - nh(a+b) + ab] \\
\tau_{SB_n} &\simeq \frac{2}{Lc}[n^2h^2 - nh(b-a)] \\
\tau_{BS_n} &\simeq \frac{2}{Lc}[n^2h^2 - nh(a-b)] \\
\tau_{BB_n} &\simeq \frac{2}{Lc}[(n-1)^2h^2 + (n-1)h(a+b) + ab] \qquad (5)
\end{aligned}$$

3) Combined Multipath Channel Response: For the channel structure shown in Fig 2, the received signal $r(t)$ constructed in terms of the summation of image signals is given by:

$$\begin{aligned}
r(t) = \frac{e^{j\omega(t-t_D)}}{D}\{1 &+ \sum_{n=1}^{\infty}[\alpha_{ss_n}e^{-\tau_{ss_n}} + \alpha_{sb_n}e^{-\tau_{sb_n}} \\
&+ \alpha_{bs_n}e^{-\tau_{bs_n}} + \alpha_{bb_n}e^{-\tau_{bb_n}}]\} \qquad (6)
\end{aligned}$$

In the computation of (6), we can limit the number of terms to include only those with significant amplitudes. In our simulations, we neglect terms smaller than 2% of the amplitude of the direct path signal.

B. Noise Modeling

The channel model includes models for ambient and significant intermittent noise sources. Ambient noise sources include surface agitation noise, and thermal nose. Intermittent noise sources include noise due to snapping shrimp and rain noise.

1) Surface Agitation Noise: The noise caused by the bursting of bubbles of dissolved air at the air-water interface, gives rise to noise which is mainly dependant on wind speed [11].

$$N_{wind} = 20.5 + 22.4 \log U \qquad (7)$$

where U is the wind speed in m/s at a reference height of 10m above the surface of the water.

The frequency dependent ambient noise level due to surface agitation can be given by [13]

$$N_{surface\ agitation} = N_{wind} + 20.7 - 15.9 \log f \qquad (8)$$

where f is the frequency in kHz.

2) Thermal Noise: The noise due to the thermal excitation of the water can be modeled by [12]

$$N_{thermal} = -15 + 20 \log f \qquad (9)$$

where f is the frequency in kHz.

3) Noise due to Snapping Shrimp: There are currently no theoretical models for modeling the noise due to snapping shrimp [11]. The empircial formula developed by Urick [12] for modeling noise due to snapping shrimp is

$$N_{shrimp} = -15 + 20 \log f \qquad (10)$$

where f is the frequency in kHz.

4) Rain Noise: The noise level for rain is a function of the size and velocity of the water droplets when they hit the water surface. Both of these factors are dependent on the rate of rainfall [12]. The noise due to rain is a combined effect of the wind speed and the rain rate [13].

$$N_{rain} = b + a \log RR \qquad (11)$$

where

$$\begin{array}{ll}
a = 25.0 & U \leq 1.5 \\
a = 5.0 + 5.7(5.0 - U) & 1.5 < U < 5.0 \\
a = 5.0 & U \geq 5.0
\end{array} \qquad (12)$$

and

$$\begin{array}{ll}
b = 41.6 & U \leq 1.5 \\
b = 50.0 + 2.4(5.0 - U) & 1.5 < U < 5.0 \\
b = 50.0 & U \geq 5.0
\end{array} \qquad (13)$$

RR is the rain rate in mm/h, and U is the wind speed in m/s.

III. Multiuser CDMA

CDMA is a spread spectrum communications scheme that is capable of supporting multiple users simultaneously within the same bandwidth. Each user is assigned a unique high-rate spreading sequence which is used to modulate the transmitted data stream.

Since all the users share the same transmission media, the transmit signals from different users become superimposed at the receiver, causing multiple access interference (MAI). At the receiver side, multi-user detection (MUD) techniques are used to separate the mixed signals and decode the transmit data from each of the users.

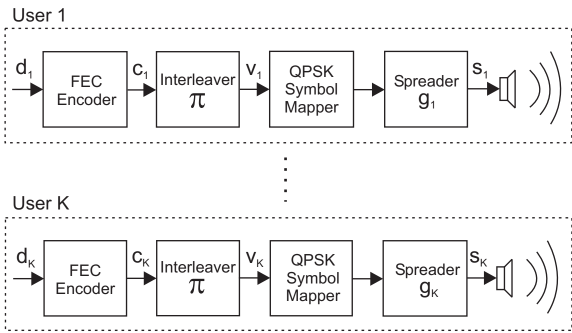

Fig. 3. Transmitter structure for the multiuser CDMA system

Fig 3 shows the transmitter structure of the multiple access CDMA scheme with K simultaneous users. Let k be the user index. Each user k is assigned a unique signature sequence g_k (with length G). The elements in g_k are commonly called chips. Data from user k is first encoded by a rate-R binary forward error control (FEC) code followed by interleaving. Here interleaving is mainly to alleviate the fading effect. The spreader for user k then spreads a coded bit into a sequence of G chips.

The spreading operation produces redundancy, and therefore bandwidth expansion, since a single chip alone can carry one bit of information. This redundancy is used to distinguish different users, but from a coding perspective, this is not ideal since the redundancy is introduced without coding gain.

IV. Multiuser IDMA

IDMA is a multiple access scheme in which interleaving is the only means of user separation, As a special form of CDMA, IDMA inherits many advantages of CDMA, such as dynamic channel sharing, asynchronous transmission, and robustness against fading. Furthermore, it allows a low-cost interference cancelation technique applicable to systems with large numbers of users in multipath channels.

The IDMA transmitter structure is shown in Fig 4. This can be viewed as a special case of Fig 3 when all signature sequences reduce to a single chip (i.e., $G = 1$) and therefore the spreaders can be removed. Each user is assigned a unique sequence of interleaving indexes. It is a special form of CDMA if we view each (uniquely) interleaved version of a code as a different code.

The bandwidth expansion is entirely achieved by a low-rate FEC code. This code can be a combination of a repetition code (for bandwidth expansion) and a stronger code (for coding gain), which provides a trade-off between performance and complexity.

A. IDMA Transmitter Structure

Fig 4 shows the transmitter structure of the multiple- access IDMA scheme with K simultaneous users [5]. The input data

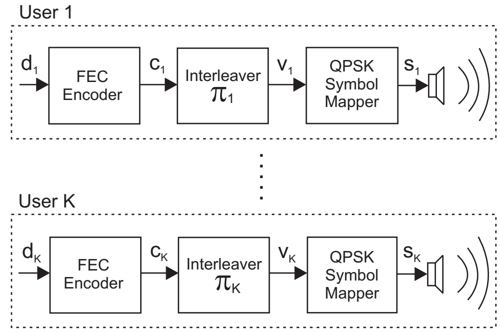

Fig. 4. Transmitter structure for the multiuser IDMA system

sequence $\mathbf{d}_k$ of user-k is encoded by the FEC encoder generating a coded sequence $\mathbf{c}_k \equiv [c_k(1), \ldots, c_k(j), \ldots c_k(J)]^T$, where J is the frame length. The elements in $\mathbf{c}_k$ are referred to as coded bits. Then $\mathbf{c}_k$ is permutated by the interleaver π_k, producing $\mathbf{v}_k \equiv [v_k(1), \ldots, v_k(j), \ldots v_k(J)]^T$. Finally, the interleaved chip sequence is QPSK modulated, producing $\mathbf{s}_k$. The elements of $\mathbf{s}_k$ are referred to as chips in accordance with CDMA convention.

A key principle of IDMA is that users are distinguished solely by their interleaver sequence, and therefore the interleaver π_k must be different for each user. The interleavers are assumed to be generated randomly and independently. These interleavers disperse the coded sequences so that the adjacent chips are approximately uncorrelated.

B. Signal Model

We consider the case of underwater acoustic channels with memory due to multipath delay dispersion. Each received sample can be expressed using an L-tap model as

$$r(j) = \sum_{k=1}^{K} \sum_{l=0}^{L-1} h_k(l) s_k(j-l) + n(j) \tag{14}$$

where $s_k(j)$ is the j-th chip transmitted by user k, $h_k(l)$ is the channel coefficient for user k (corresponding to a delay of l chip durations), and $n(j)$ is a noise sample. For a particular user k, we can rewrite (14) as

$$r(j) = h_k(l) s_k(j-l) + \zeta_{k,l}(j) \tag{15}$$

where $\zeta_{k,l}(j)$ is the distortion (including additive noise, interference from other users as well as ISI from the same user) contained in $r(j)$ with respect to $s_k(j-l)$.

C. Iterative Receiver Structure

We consider the joint multiple-access system with FEC coding in Fig 4 as a serially concatenated coding system, in which the FEC code takes the role of the outer code, and the multiple-access channel takes the role of the inner code. Using this interpretation, an iterative receiver structure can developed where soft information is exchanged between the multiuser detector (MUD) and the FEC decoders [14] .

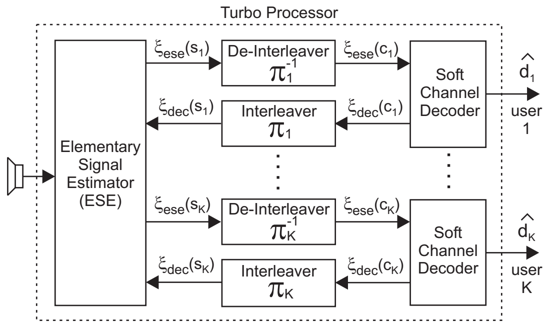

Fig. 5. Receiver structure for the multiuser IDMA system

The iterative receiver structure for the multiuser IDMA system is shown in Fig 5. It consists of a soft-output elementary signal estimator (ESE) and K single users *a posteriori* probability decoders (DECs). The two stages are separated by by interleavers and deinterleavers. The soft-output ESE takes as input the received signals and the interleaved extrinsic log likelihood ratios (LLRs) of the code bits of all users (which are fed back by the K single-user DECs), and computes as the output the a posteriori LLRs of the code bits of all users. The DEC of *k*th users takes as input the deinterleaved extrinsic LLRs of the code bits from the soft-output ESE and computes as output the *a posteriori* LLRs of the code bits, as well as the LLRs of the information bits.

This turbo-type iterative process is sub-optimal as the multiple access and FEC coding constraints are considered separately, however this approach has greatly reduced complexity compared to optimal detection approaches.

We next describe each component of the receiver.

D. Elementary Signal Estimator (ESE)

The ESE is developed from the concepts described in [5]. At a given iteration, the ESE estimates the *a posteriori* LLRs of the code bits $s_k(j)$

$$\ell_{ese}(s_k(j)) \triangleq \log \frac{P(s_k(j)=1 \mid \mathbf{r})}{P(s_k(j)=0 \mid \mathbf{r})} \tag{16}$$

for $j = 1, \ldots, J$, and $k = 1, \ldots, K$. Here, $\mathbf{r}$ denotes the received vector. (Note that the real and imaginary components of s_k are decoded independently.)

With Bayes' rule, (16) can be rewritten as

$$\ell_{ese}(s_k(j)) = \log \frac{P(\mathbf{r} \mid s_k(j)=1)}{P(\mathbf{r} \mid s_k(j)=0)} + \log \frac{P(s_k(j)=1)}{P(s_k(j)=0)} \tag{17}$$

The first term is the extrinsic information calculated by the ESE and is denoted as $\xi_{ese}(s_k(j))$

$$\xi_{ese}(s_k(j)) = \log \frac{P(\mathbf{r} \mid s_k(j)=1)}{P(\mathbf{r} \mid s_k(j)=0)} \tag{18}$$

The second term in (17) is the *a priori* LLR of $s_k(j)$. An estimate of this term is calculated by the DEC of the *k*-th user at the previous iteration. At the first iteration, no prior information about the code bits is available, therefore all bit values are assumed equiprobable and the *a priori* LLR values are set to zero. Finally, the sequence of extrinsic information $\xi_{ese}(s_k(j))$ is deinterleaved by the deinterleaver of the *k*th user and fed into the corresponding DEC as *a priori* information for the next iteration.

The calculation of the extrinsic information for each user is now described in more detail. By rewriting (15), the received signal from user-k via path-l can be described as

$$r(j+l) = h_k(l)s_k(j) + \zeta_{k,l}(j) \tag{19}$$

Denote the conjugate of $h_k(l)$ by $h_k^*(l)$ and generate

$$\tilde{r}(j+l) = h_k^*(l)r(j+l) = |h_k(l)|^2 x_k(j) + \tilde{\zeta}_{k,l}(j) \tag{20}$$

where

$$\tilde{\zeta}_{k,l}(j) = h_k^*(l)\zeta_{k,l}(j) \tag{21}$$

By the central limit theorem, $\tilde{\zeta}_{k,l}(j)$ can be approximated as a Gaussian variable. The phase shift due $h_k(l)$ is canceled out in (20), which means that the real and imaginary parts of $s_k(j)$ can be decoded independently. This reduces the complexity of decoding the QPSK mapping. The extrinsic information for user-k and path-l can be written as

$$\begin{aligned} \xi_{ese}(s_k(j))_l &= \log \frac{P(\tilde{r}(j+l) \mid s_k(j)=1)}{P(\tilde{r}(j+l) \mid s_k(j)=0)} \\ &= 2|h_k(l)|^2 \frac{\tilde{r}(j+l) - \mathrm{E}\left(\tilde{\zeta}_k(j)\right)}{\mathrm{Var}\left(\tilde{\zeta}_k(j)\right)} \end{aligned} \tag{22}$$

where $\mathrm{E}(.)$ and $\mathrm{Var}(.)$ are the mean and variance functions, respectively. Finally, the extrinsic information for user-k, considering all l-paths of the channel can be written as

$$\xi_{ese}(s_k(j)) = \sum_{l=0}^{L-1} \xi_{ese}(s_k(j))_l \tag{23}$$

E. Soft Channel Decoding (DEC)

The channel decoder for the *k*-th user estimates the *a posteriori* LLR of the code bits

$$\ell_{dec}(s_k(j)) \triangleq \log \frac{P(s_k(j)=1 \mid \mathbf{r})}{P(s_k(j)=0 \mid \mathbf{r})} \tag{24}$$

based on the extrinsic information from the ESE, and knowledge of the code structure. To estimate the $\ell_{dec}(s_k(j))$, the FEC (convolutional) code is soft-decoded by the BCJR algorithm [15]. As in (17), $\ell_{dec}(s_k(j))$ can be expressed as the sum of extrinsic information $\xi_{dec}(s_k(j))$ and an *a priori* LLR. The sequence of extrinsic information is interleaved and fed back to the MUD as *a priori* information for the next iteration. Additionally, the DEC estimates the *a posteriori* LLRs of the information bits, and at the final iteration, performs a hard decision on the information bits.

V. Multiuser OFDM-IDMA

The basic principle of multicarrier modulation is to split a high-rate data stream into a number of lower rate streams that are transmitted simultaneously over a number of sub-carriers. Because the symbol duration increases for the lower rate parallel subcarriers, the relative amount of dispersion in time caused by multipath delay spread is decreased. The bandwidth of each is sufficiently narrow so that the frequency response characteristics of the subchannels are nearly flat [16].

OFDM is an efficient realization of multicarrier modulation communication in which the subcarriers are made mutually orthogonal. The attribute of orthogonality allows the subcarrier spectra to overlap, while still allowing the subcarrier signals to be received without adjacent carrier interference.

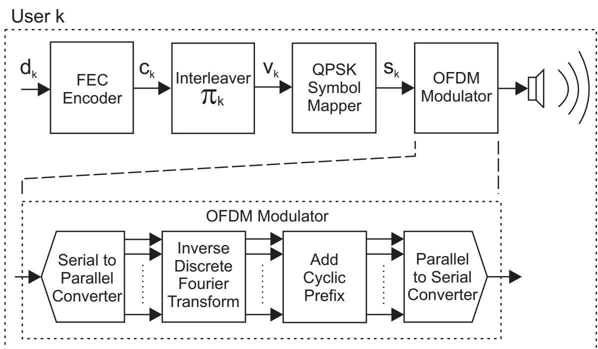

Fig. 6. Transmitter structure for the multiuser MC-IDMA system

Consider an OFDM system with N_c subcarriers. The frequency spacing of the N_c subcarriers is $\triangle f$. The total system bandwdith B is divided into N_c equidistant subchannels. All subcarriers will be mutually orthogonal within a time interval of length $T_s = 1/\triangle f$. The n-th subcarrier signal is described analytically by the function $\tilde{x}_n(t),\ n = 0, 1, , \dots N_c - 1$.

$$\tilde{x}_n(t) = \begin{cases} e^{i2\pi n \triangle f t} & \text{for } 0 \leq t \leq T_S \\ 0 & \text{otherwise} \end{cases} \tag{25}$$

Since the system bandwidth B is subdivided into N narrowband channels, the OFDM block duration T_S is N times as large as in the case of a single-carrier transmission system covering the same bandwidth. Typically, for a given system bandwidth, the number of subcarriers is chosen such that the symbol duration is large compared to the maximum delay of the channel. The subcarrier signal $\tilde{x}_n(t)$ is extended by a cyclic prefix (called guard interval) with the length T_G yielding the following signal

$$x_n(t) = \begin{cases} e^{i2\pi n \triangle f t} & \text{for } -T_G \leq t \leq T_S \\ 0 & \text{otherwise} \end{cases} \tag{26}$$

The cyclic prefix is added to the subcarrier signal in order to reduce or eliminate ISI from a multipath channel. At the receiver, the cyclic prefix is removed and only the time interval $0 \leq t \leq T_S$ is evaluated. The total OFDM block duration is $T = T_S + T_G$.

The modulator and demodulator in an OFDM system can be implemented by use of a bank of filters based on the discrete Fourier transform (DFT). To improve implementation efficiency, the fast Fourier transform (FFT) algorithm is generally used to compute the DFT.

Fig 6 shows the transmitter structure of the MC-IDMA scheme using OFDM. After IDMA processing (FEC encoding, interleaving and symbol mapping), a serial to parallel (S/P) buffer sub-divides the chip sequence into N_c substreams. Then each substream is modulated onto a sub-carrier by IFFT operation. Finally, the cyclic prefix is added.

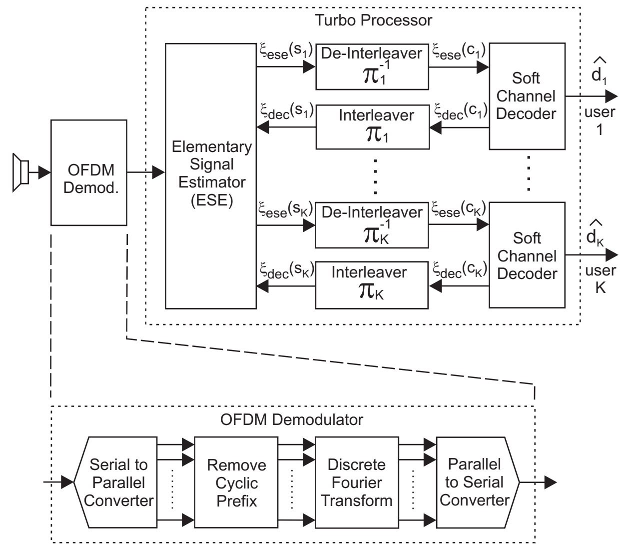

Fig. 7. Receiver structure for the multiuser MC-IDMA system

Fig 7 shows the receiver structure of the MC-IDMA scheme. OFDM demodulation is performed before iterative multiuser detection. In this scheme, ISI and MAI are independently processed by the OFDM demodulator and the ESE, respectively.

VI. Multiuser MIMO-OFDM-IDMA

MIMO (Multiple-Input and Multiple-Output) is a general term that refers to communication systems where each transmitter and receiver use multiple transmitting and receiving elements respectively. These systems exploit the spatial diversity of the multipath transmission channel underwater channel to provide improved performance in the form of either increased data robustness or increased data throughput.

MIMO transmitters use Space-Time Block Codes (STBCs) to map the input data stream into multiple sub-streams that are dispersed in linear combinations over space (i.e., transmit elements) and time.

A STBC is defined by a $(P \times N)$ code matrix $\mathcal{G}$, where N denotes the number of transmit antennas or the *spatial* transmitter diversity order, and P denotes the number of channel usages for transmitting a STBC codeword or the *temporal* transmitter diversity order.

The STBC encoder takes as input a code vector, **s**, and transmits each row of symbols as specified in $\mathcal{G}$ at P consecutive channel usages. At each channel usage, the symbols contained in the N-dimensional row vector of $\mathcal{G}$ are transmitted through N transmitter antennas simultaneously [17].

As an example, consider the 2×2 Alamouti STBC (ie., $P = 2, N = 2$) [18]. The Alamouti STBC matrix $\mathcal{G}$ is defined by

$$\mathcal{G} = \begin{bmatrix} s(1) & s(2) \\ -s^*(2) & s^*(1) \end{bmatrix} \tag{27}$$

where $(\cdot)^*$ denotes the complex conjugate operation. The input to this STBC is the code vector $\mathbf{s} = [s(1), s(2)]^T$. During the first channel use, the two symbols of the top row of $\mathcal{G}$, $[s(1), s(2)]$, are transmitted simultaneously from the two transmit elements; and during the second channel use, the symbols in the second row of $\mathcal{G}$, $[-s^*(2), s^*(1)]$, are transmitted.

In this paper, we restrict our investigation to 2×2 MIMO systems (transmitters and receivers with 2 transmitting and 2 receiving elements respectively), using the Alamouti STBC (27).

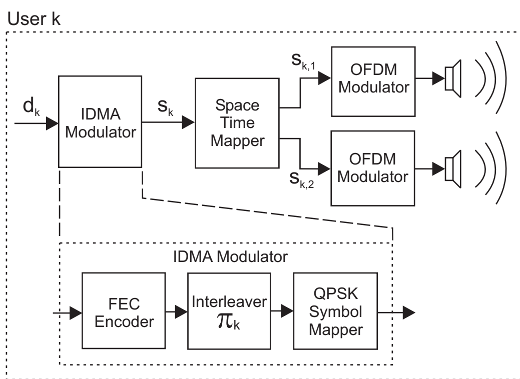

Fig. 8. Transmitter structure for the multiuser MIMO-OFDM-IDMA system

Fig 8 shows the transmitter structure of the MIMO-OFDM-IDMA scheme. The input data sequence is encoded and interleaved by the FEC encoder and interleaver respectively. The interleaved chip sequence is then QPSK-modulated followed by space-time mapping as specified by the Alamouti code matrix, $\mathcal{G}$. The Alamouti STBC provides diversity gain (compared to a single-input single-output systems). Finally, each STBC output sub-stream is independently OFDM modulated.

The channel model for the MIMO system is shown in Fig 9. For simplicity the multipath signals are not shown.

VII. Simulation Results

The system performance of the four communications schemes (CMDA, IDMA, OFDM-IDMA, and MIMO-OFDM-IDMA) are evaluated using the channel models described in section II. Each schemes is simulated with 8 simultaneous users over five different channel ranges.

The parameters for the five channel models are shown in Fig 10. The range (L) between the receiver and each transmitter is randomly selected between the minimum and maximum values listed to ensure each user has different

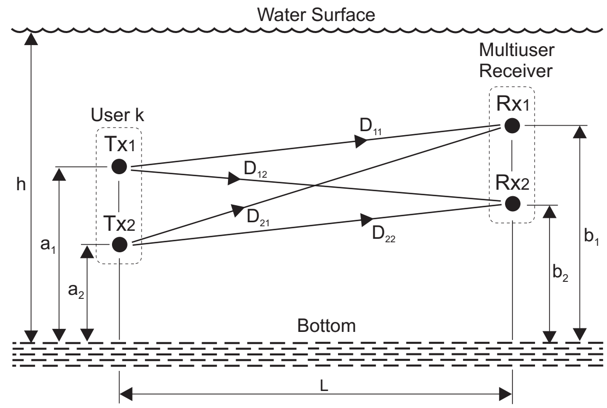

Fig. 9. Shallow water channel model for a 2 x 2 MIMO system

Channel Model	Range, L (m) min.	nom.	max.	Depth, h (m)	SNR (dB)
1	72	80	88	16	25.4
2	117	130	143	16	21.5
3	504	560	616	16	22.6
4	936	1040	1144	16	19.4
5	1359	1510	1661	16	15.1

Fig. 10. Simulation Channel Model Parameters

multipath channel characteristics. The transmitter and receiver heights are 6m and 11m respectively (i.e., $a = 6, b = 11$). For the MIMO systems, $a_1 = 5$, $a_2 = 7$, $b_1 = 10$, and $b_2 = 12$.

In each scheme, the transmitter FEC is a 1/2-rate convolutional code serially concatenated with a 1/16-rate repetition code (producing an overall code rate of $R = 1/32$). Each transmitter generates QPSK symbols and has a symbol rate of 1200 symbols per second (producing an aggregate rate of 9600 symbols per second). The OFDM systems uses 128 subcarriers.

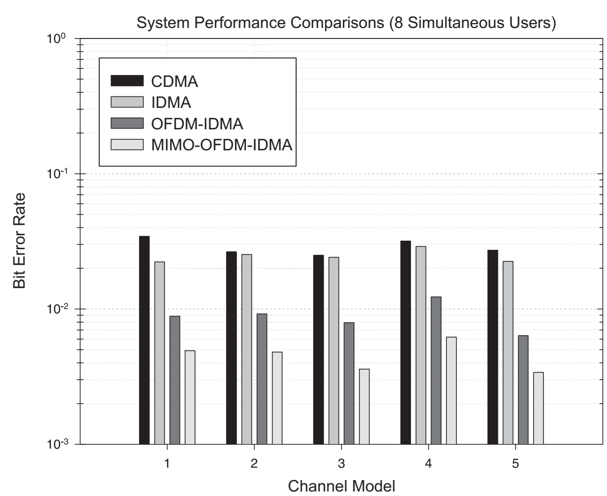

Fig. 11. System Performance Comparisons for 8 Simultaneous Users

Fig 11 compares the bit error rate (BER) averaged over all eight users for each communication scheme. We observe that the IDMA scheme provides a very modest improvement in BER performance when compared to the CDMA scheme. However, more significant BER performance improvements are observed for the OFDM- IDMA and MIMO-OFDM-IDMA schemes when compared to CDMA. The MIMO-OFDM-IDMA scheme provides the best performance, with results showing a reduction in BER of 86% compared to CDMA at a range of 1510m (Channel Model No. 5).

VIII. Conclusion

Simulation results show that for a shallow water environment, the proposed OFDM-IDMA scheme offers superior performance when compared against the other evaluated multiple-access schemes. The MIMO extension to the OFDM-IDMA scheme provides further performance improvement, but at the expense of additional transmitter and receiver complexity. The results demonstrate that MIMO-OFMD-IDMA is a strong candidate for shallow water acoustic network communication schemes, and is worthy of further research.

References

[1] D.B. Kilfoyle, and A.B. Baggeroer, " The state of the art in underwater acoustic telemetry", *IEEE Journal of Oceanic Engineering*, vol. 25, no. 1, pp 4-27, Jan. 2000

[2] C. Boulanger, G. Loubet, and J. R. Lequepeys, " Spreading sequences for underwater multiple-access communications", *OCEANS '98 Conference Proceedings*, vol. 2, pp 1038-1042 vol.2, 28 Sep.-1 Oct. 1998.

[3] C. C. Tsimenidis, O. R Hinton, A. E. Adams, and B. S. Sharif, "Underwater acoustic receiver employing direct-sequence spread spectrum and spatial diversity combining for shallow-water multiaccess networking", *IEEE Journal of Oceanic Engineering*, vol. 26, no. 4, pp 594-603, Oct. 2001.

[4] M. Stojanovic, and L. Freitag, "Multiple Detection for Wideband Underwater Acoustic CDMA Communications", *IEEE Journal of Oceanic Engineering*, vol. 31, no. 3, pp 685-695, July 2006.

[5] L. Ping, L. Liu, K. Wu, and W. K. Leung, "Interleave-divison multiple-access", *IEEE Transactions on Wireless Communications*, vol. 5, no. 4, pp 938 - 947, Apr. 2006

[6] R. H. Mahadevappa, and J. G. Proakis, "Mitigating multiple access interfence and intersymbol interference in uncoded CDMA systems with chip-level interleaving", *IEEE Transactions on Wireless Communications*, vol. 1, no. 10, pp 781 - 792, Oct. 2002.

[7] C. Berrou, and A. Glavieux, "Near optimum error coding and decoding: Turbo-codes", *IEEE Transactions on Communications*, vol. 44, no. 10, pp 1261-1271, Oct. 1996.

[8] P. C. Etter, "Underwater Acoustic Modeling and Simulation, 3rd ed.", Spon Press, London, UK, 2003.

[9] A. Zielinski, Y.-H. Yoon, and L. Wu, " Performance analysis of digital acoustic communication in a shallow water channel", *IEEE Journal of Oceanic Engineering*, vol. 20, iss. 4, pp 293-299, Oct. 1995.

[10] J. G. Proakis, "Digital Communications", McGraw-Hill, New York, USA, 2001.

[11] S. R. Govilkar, "A simulator for the microcontroller-based underwater ultrasonic communications", M.Sci. Thesis, North Carolina State University, Raleigh, North Carolina, USA, 2006.

[12] R. J. Urick, "Ambient noise in the sea" Naval Sea Systems Commnad, Department of the Navy, Washington DC, USA, 1984.

[13] University of Washington Applied Physics Laboratory, "Apl-uw high-frequency ocean environmental acoustic models handbook", Technical report, Applied Physic Laboratory, Univeristy of Washington, Seattle WA, USA, 1994.

[14] C. Schlegel, and A. Grant, "Coordinated Multiuser Communications", Dordrecht, The Netherlands: Springer, 2006.

[15] L. R. Bahl, J. Cocke, F. jelinek, and J. Raviv,"Optimal decoding of linear codes for minimizing symbol error rate", *IEEE Transactions on Information Theory*, vol. 20, pp 284-287, Mar. 1974.

[16] R. van Nee, and R. Prasad, "OFDM for wireless multimedia communications", Artech House, Boston, USA, 2000.

[17] V. Tarokh, N. Seshadri, and A.R. Calderbank, "Space-time codes for high data rate wireless communication: performance criterion and code construction", *IEEE Transactions on Information Theory*, vol. 44, no. 2, pp 744-765, Mar. 1998.

[18] S. M. Alamouti, "A simple transmit diversity technique for wireless communications", *IEEE Journal on Selected Areas in Communications*, vol. 16, no. 8, pp 1451 - 1458, Oct. 1998.